Recherches sur le bruit des éoliennes à l'IMSIA

Benjamin Cotté

Institute of Mechanical Sciences and Industrial Applications
ENSTA Paris, Institut Polytechnique de Paris
benjamin.cotte@ensta-paris.fr

Journée GDR EOL-EMR – 25 Novembre 2021

Institut des Sciences de la Mécanique et Applications Industrielles (IMSIA)

- UMR CNRS - ENSTA Paris - EDF - CEA (directeur : H. Maitournam)
- 42 chercheurs, $\approx$ 50 doctorants/postdocs
- Spécificités :
  - laboratoire de mécanique des fluides et des solides, qui va de la recherche fondamentale aux applications industrielles
  - moyens expérimentaux à l'échelle du laboratoire et à l'échelle industrielle
  - codes industrielles : Code_Saturne, Code_Aster, CAST3M, Europlexus...

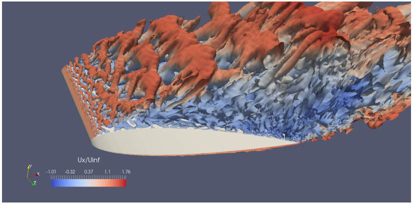

Isocontours du critère Q pour un NACA 0012 à un angle d'attaque de 20° et Reynolds 2×10^5 (LES Code_Saturne)

IMSIA : moyens expérimentaux en mécanique des fluides et acoustique

- 4 souffleries et 1 tunnel de cavitation

- 1 chambre anéchoïque

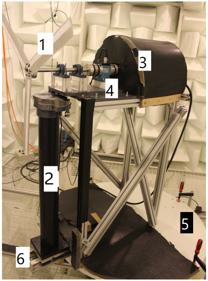

IMSIA : impact du déferlement des vagues sur les structures offshore

Projets de Luc Pastur en collaboration avec le LHSV, le CEREMA et EDF R&D autour des points suivants :

1. propagation des vagues irrégulières
2. caractérisation et statistiques de déferlement de vagues
3. efforts sur la structure (mono-pile).

Contexte : bruit des éoliennes

- Contraintes réglementaires :
  - critères d'émergence : 5 dB(A) le jour et 3 dB(A) la nuit en France
  - niveaux absolus : 39 ou 44 dB(A) en fontion des zones au Danemark
- Gêne pour des niveaux plus faibles que d'autres sources de bruit

  ⇒ contenu basse fréquence et modulations d'amplitude du bruit
- Modulations d'amplitude audibles près de l'éolienne, et parfois à grande distance en fonction des conditions météorologiques.

Contexte : bruit des éoliennes

- Contraintes réglementaires :
  - critères d'émergence : 5 dB(A) le jour et 3 dB(A) la nuit en France
  - niveaux absolus : 39 ou 44 dB(A) en fontion des zones au Danemark
- Gêne pour des niveaux plus faibles que d'autres sources de bruit

  ⇒ contenu basse fréquence et modulations d'amplitude du bruit
- Modulations d'amplitude audibles près de l'éolienne, et parfois à grande distance en fonction des conditions météorologiques.

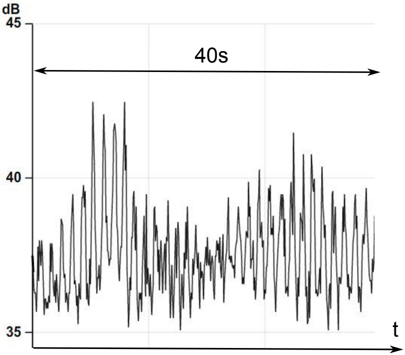

wind turbine measurement in Wadlow (UK) by MAS environmental (`www.masenv.co.uk`)

Amplitude modulation of wind turbine noise

Example of amplitude modulation measured by Dick Bowdler (`www.dickbowdler.co.uk`) 50 m upwind of a 93 m diameter WT

Swish to Thump

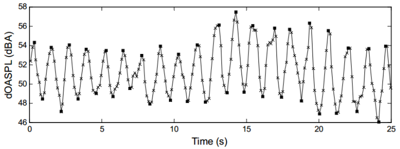

Spectrogram of this measurement (Smith *et al.* [2012])

Transition from “normal swish” to “thump”

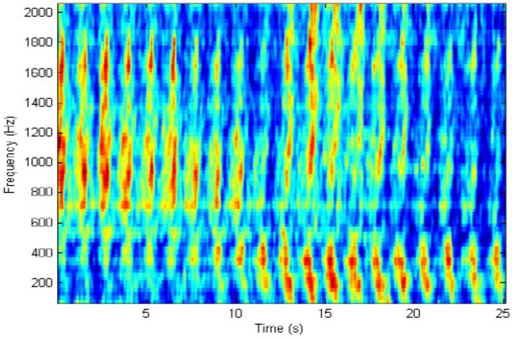

Outline

1. Wind turbine noise sources
   - modeling of broadband aerodynamic noise using Amiet's theory
   - application to a three-bladed wind turbine and auralization
   - experimental characterization of dynamic stall noise on a pitching airfoil
2. Modeling of wind turbine noise propagation effects
   - point source approximation and extended source models
   - predictions of overall sound pressure level and amplitude modulation in a neutral atmosphere

Main wind turbine aeroacoustic sources

- broadband aeroacoustic sources
  - turbulent inflow noise
  - turbulent boundary layer trailing edge noise
  - separation/stall noise

⇒ could be the cause of enhanced amplitude modulations (Oerlemans [2013])

Brooks, Pope and Marcolini (1989)

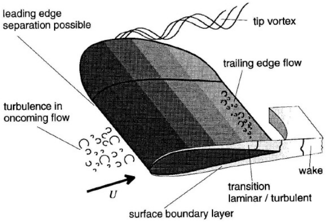

Wagner [1996]

Bertagnolio *et al.* [2015]

Main wind turbine aeroacoustic sources

- broadband aeroacoustic sources
  - turbulent inflow noise
  - turbulent boundary layer trailing edge noise
  - separation/stall noise

⇒ could be the cause of enhanced amplitude modulations (Oerlemans [2013])

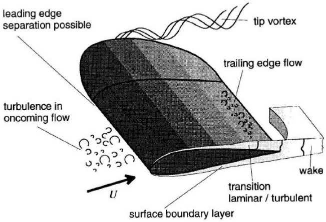

Wagner [1996]

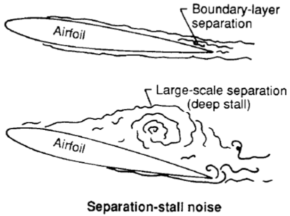

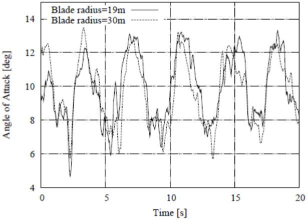

Brooks, Pope and Marcolini (1989)

Bertagnolio *et al.* [2015]

Amiet theory for a fixed airfoil

Far-field PSD of acoustic pressure for trailing edge noise calculated for $L/c > 3$

$$S_{pp}^F(\mathbf{x_R}, \omega) = \left(\frac{\omega c z_R}{4\pi c_0 S_0^2} \right)^2 2L \left| \mathcal{I}\left(\frac{\omega}{U_c}, \mathbf{x_R} \right) \right|^2 \Phi_{pp}(\omega) l_y(\omega)$$

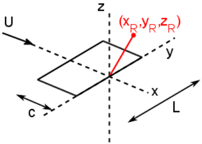

$\left| \mathcal{I}\left(\frac{\omega}{U_c}, \mathbf{x_R} \right) \right|^2$: aeroacoustic transfer function
$\Phi_{pp}(\omega)$: PSD of wall pressure fluctuations
$l_y(\omega)$: spanwise correlation length

Trailing edge noise directivity :

- $f = 16\,\text{Hz}$ $(kc = 0.2)$
- $f = 50\,Hz (kc = 0.7)$
- $f = 120\,Hz (kc = 1.8)$
- $f = 500\,Hz (kc = 7.2)$

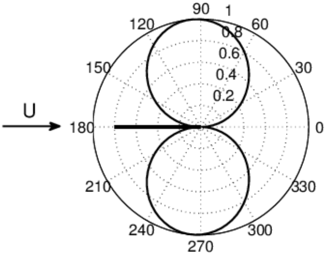

Amiet theory for a fixed airfoil

Far-field PSD of acoustic pressure for trailing edge noise calculated for $L/c > 3$

$$S_{pp}^F(\mathbf{x_R}, \omega) = \left(\frac{\omega c z_R}{4\pi c_0 S_0^2}\right)^2 2L \left|\mathcal{I}\left(\frac{\omega}{U_c}, \mathbf{x_R}\right)\right|^2 \Phi_{pp}(\omega) l_y(\omega)$$

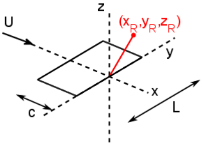

$\left|\mathcal{I}\left(\frac{\omega}{U_c}, \mathbf{x_R}\right)\right|^2$: aeroacoustic transfer function

$\Phi_{pp}(\omega)$: PSD of wall pressure fluctuations

$l_y(\omega)$: spanwise correlation length

Trailing edge noise directivity :

- $f = 16\,\text{Hz}$ $(kc = 0.2)$
- $f = 50\,Hz (kc = 0.7)$
- $f = 120\,Hz (kc = 1.8)$
- $f = 500\,Hz (kc = 7.2)$

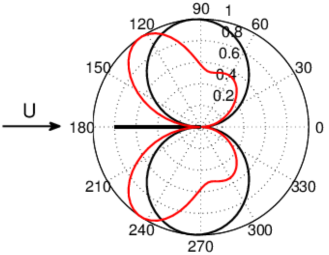

Amiet theory for a fixed airfoil

Far-field PSD of acoustic pressure for trailing edge noise calculated for $L/c > 3$

$$S_{pp}^F(\mathbf{x_R},\omega) = \left(\frac{\omega c z_R}{4\pi c_0 S_0^2}\right)^2 2L\left|\mathcal{I}\left(\frac{\omega}{U_c},\mathbf{x_R}\right)\right|^2 \Phi_{pp}(\omega) l_y(\omega)$$

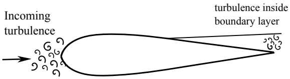

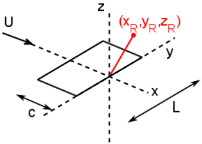

$\left|\mathcal{I}\left(\frac{\omega}{U_c},\mathbf{x_R}\right)\right|^2$: aeroacoustic transfer function

$\Phi_{pp}(\omega)$: PSD of wall pressure fluctuations

$l_y(\omega)$: spanwise correlation length

Trailing edge noise directivity :

- $f = 16\,\mathrm{Hz}$ $(kc = 0.2)$
- $f = 50\ Hz(kc = 0.7)$
- $f = 120\ Hz(kc = 1.8)$
- $f = 500\ Hz(kc = 7.2)$

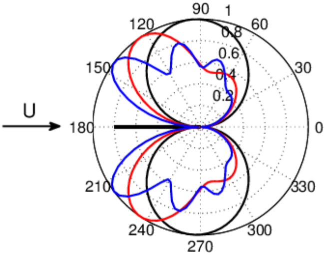

Amiet theory for a fixed airfoil

Far-field PSD of acoustic pressure for trailing edge noise calculated for $L/c > 3$

$$S_{pp}^F(\mathbf{x_R},\omega) = \left(\frac{\omega c z_R}{4\pi c_0 S_0^2}\right)^2 2L\left|\mathcal{I}\left(\frac{\omega}{U_c},\mathbf{x_R}\right)\right|^2 \Phi_{pp}(\omega) l_y(\omega)$$

$\left|\mathcal{I}\left(\frac{\omega}{U_c},\mathbf{x_R}\right)\right|^2$: aeroacoustic transfer function

$\Phi_{pp}(\omega)$: PSD of wall pressure fluctuations

$l_y(\omega)$: spanwise correlation length

Trailing edge noise directivity :

- $f = 16\,\text{Hz}$ $(kc = 0.2)$
- $f = 50\ Hz(kc = 0.7)$
- $f = 120\ Hz(kc = 1.8)$
- $f = 500\ Hz(kc = 7.2)$

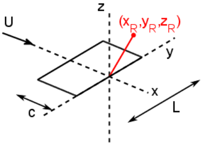

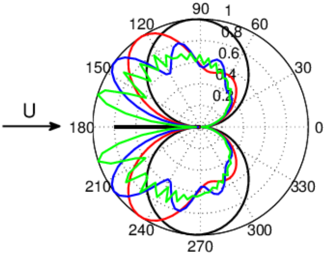

Application to a rotating blade

- each blade is divided into N_s segments (strip theory)
- For each segment at each angular position β :
  - contribution of segment at the receiver calculated using Amiet theory
  - correction due due to Doppler effect

$$S_{pp}^R(\mathbf{x_R^T}, \omega, \beta) = \frac{\omega_e}{\omega} S_{pp}^F(\mathbf{x_R^B}, \omega_e, \beta)$$

  $\mathbf{x_R^T}$: receiver coordinates in the wind turbine reference system
  $\mathbf{x_R^B}$: receiver coordinates in the blade reference system
  - logarithmic summation

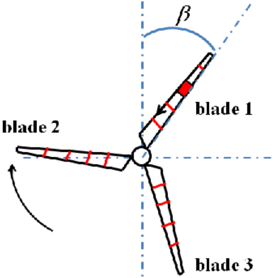

Application to a rotating blade

- each blade is divided into N_s segments (strip theory)
- For each segment at each angular position β :
  - contribution of segment at the receiver calculated using Amiet theory
  - correction due due to Doppler effect

$$S_{pp}^{R}(\mathbf{x_R^T}, \omega, \beta) = \frac{\omega_e}{\omega} S_{pp}^{F}(\mathbf{x_R^B}, \omega_e, \beta)$$

  $\mathbf{x_R^T}$: receiver coordinates in the wind turbine reference system
  $\mathbf{x_R^B}$: receiver coordinates in the blade reference system
  - logarithmic summation

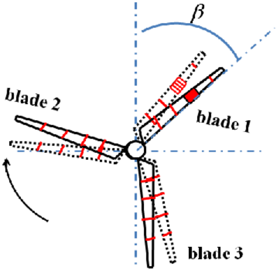

Comparison with 2.3 MW wind turbine measurements

Results of Tian and Cotté [2016]

- hub height of 80 m, rotor diameter of 93 m
- blade length 45 m, cut into 8 segments ($L/c > 3$)
- measurements performed at DTU (Leloudas [2006])

$U_{ref} = 6$ m/s

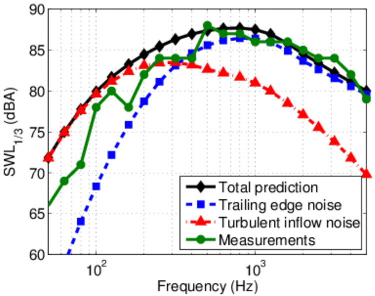

$U_{ref} = 8$ m/s

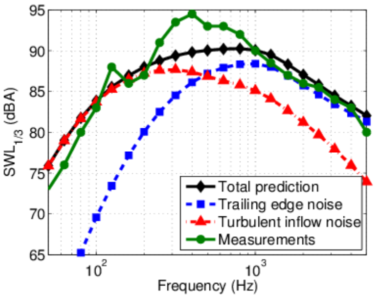

Physics-based sound synthesis

- Auralization tool built by David Mascarenhas (ITN VRACE)
- Synthesis of short grains with cross-fading to avoid clicks

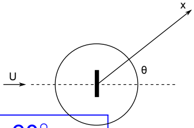

Receiver at $\theta = 0^\circ$

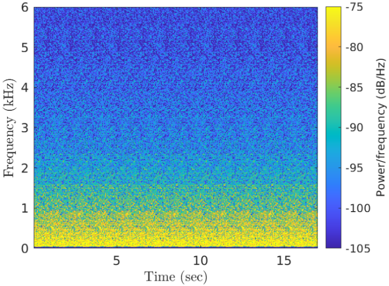

Receiver at $\theta = 90^\circ$

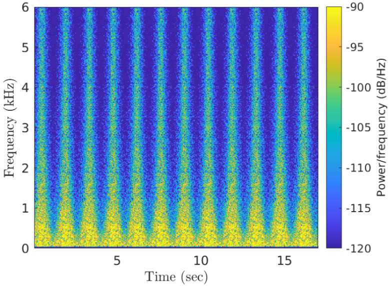

More details in WTNC conference paper by Mascarenhas, Cotté and Doaré “Physics-based auralization of wind turbine noise”

Noise emitted by an airfoil undergoing static or dynamic stall

- At stall, the noise emitted by a **static airfoil** increases significantly compared to an attached boundary layer noise (Brooks *et al.* [1989])

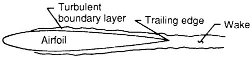

Turbulent boundary layer - trailing edge noise

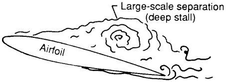

Stall noise

- The aerodynamics of **dynamic stall** is quite well known (Mulleners and Raffel [2013]) but not the associated acoustics

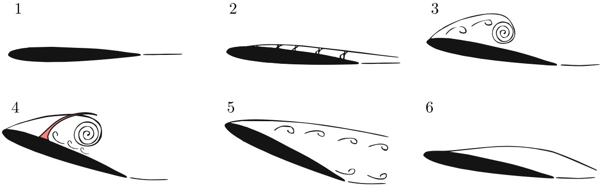

- One of the objective of the ANR project PIBE (*Prédire l'Impact du Bruit des Éoliennes*) is to characterize experimentally dynamic stall noise

Experimental setup : ECL anechoic wind-tunnel

Collaboration with Michel Roger, Emmanuel Jondeau and Pascal Souchotte from LMFA

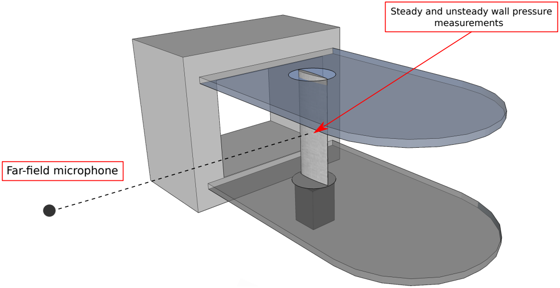

- U = 50 m/s :
  - $Re_c = Uc/\nu = 4 \cdot 10^5$
  - $Ma = U/c_0 = 0.15$
- Airfoils :

Static airfoil :

- $\alpha_{s,g} = [0^\circ, ..., 30^\circ]$

Oscillating airfoil :

- $\alpha_{d,g} = 15^\circ + 15^\circ \sin(2\pi f\ t)$
- Reduced frequency : $k = \frac{\pi fc}{U} = [0.005 - 0.025]$

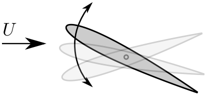

Static stall noise

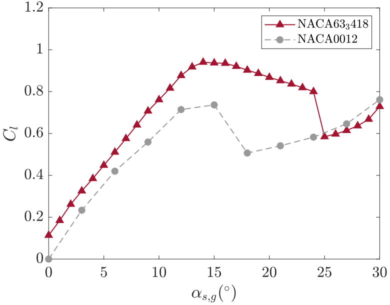

Static stall noise

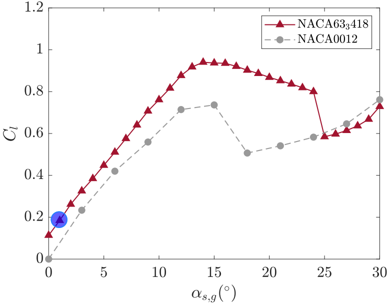

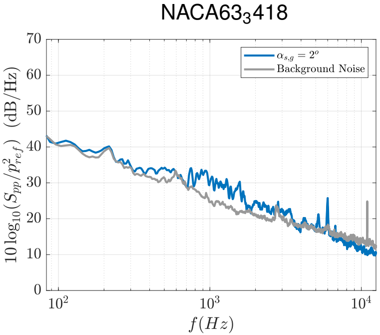

- At low angles of attack : low amplitude turbulent boundary layer trailing edge noise.

Static stall noise

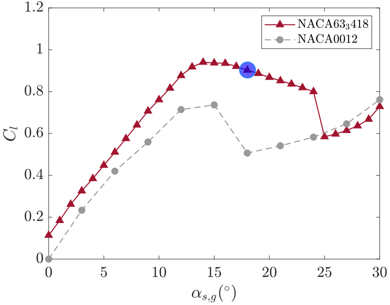

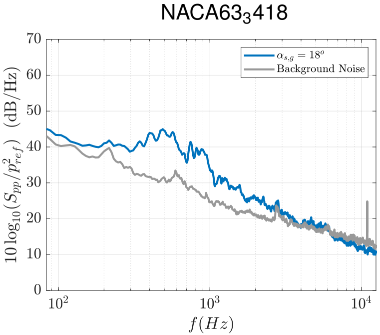

- At low angles of attack : low amplitude turbulent boundary layer trailing edge noise.
- Above stall for $\alpha_{0,g} < 27^o$: partially separated boundary layer $\Rightarrow$ broadband low frequency noise (**light-stall noise**).

Static stall noise

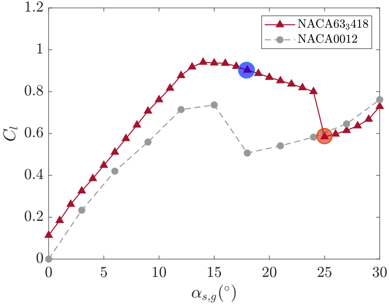

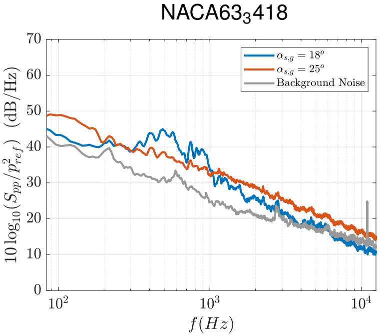

- At low angles of attack : low amplitude turbulent boundary layer trailing edge noise.
- Above stall ($\alpha_{0,g} < 27^o$) : partially separated boundary layer $\Rightarrow$ broadband low frequency noise (**light-stall noise**).

Static stall noise

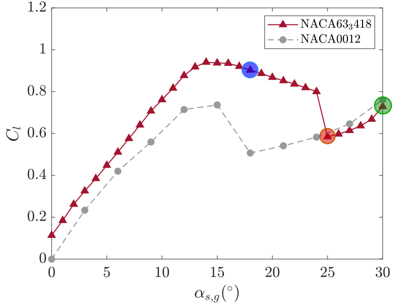

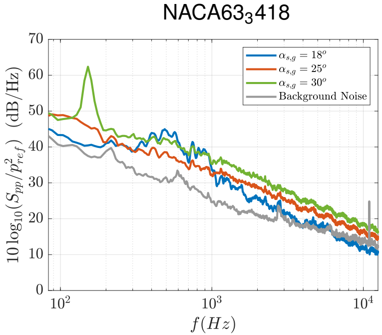

- At low angles of attack : low amplitude turbulent boundary layer trailing edge noise.
- Above stall ($\alpha_{0,g} < 27^o$) : partially separated boundary layer $\Rightarrow$ broadband low frequency noise (**light-stall noise**).
- $\alpha_{0,g} \geq 27^o$: large scale vortex shedding $\Rightarrow$ low frequency narrow-band peak (**deep-stall noise**)

Oscillating airfoil : example

$$\begin{cases} \text{NACA}63_3418 \\ \alpha_{d,g} = 15^\circ + 15^\circ \sin(2\pi f\ t) \\ U = 50\,\text{m/s} \\ f = 1.3\,\text{Hz} - k = 0.01 \end{cases}$$

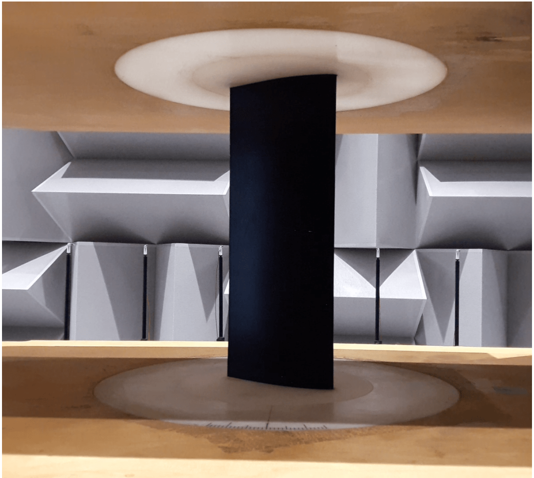

Phase-averaged spectrogram over 90 cycles

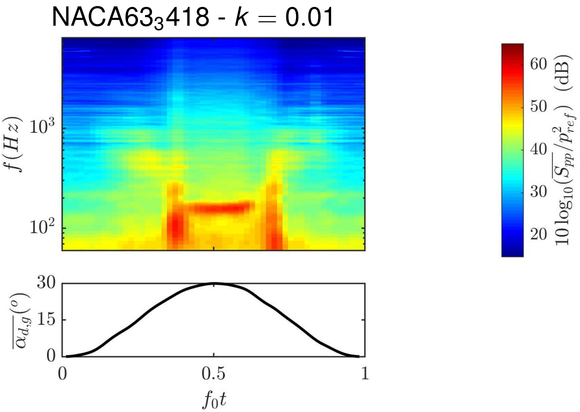

- Similar **light-stall noises** at stall onset and flow reattachment.
- **Deep-stall noise** in between.

Phase-averaged spectrogram over 90 cycles

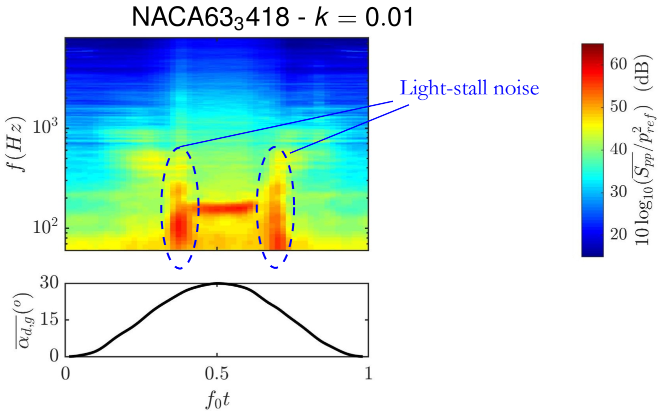

- Similar **light-stall noises** at stall onset and flow reattachment.
- **Deep-stall noise** in between.

Phase-averaged spectrogram over 90 cycles

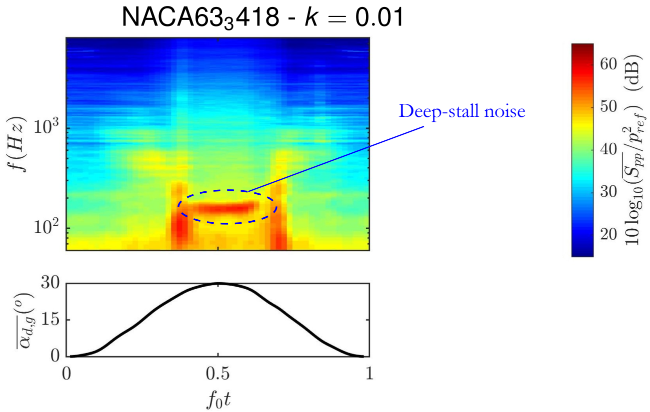

- Similar **light-stall noises** at stall onset and flow reattachment.
- **Deep-stall noise** in between.

Oscillating airfoil : effect of the reduced frequency

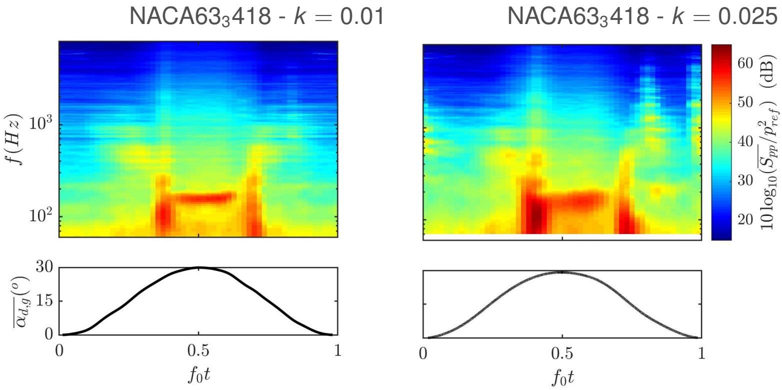

- Increase of the amplitude of the stall onset broadband noise

Oscillating airfoil : effect of the airfoil shape

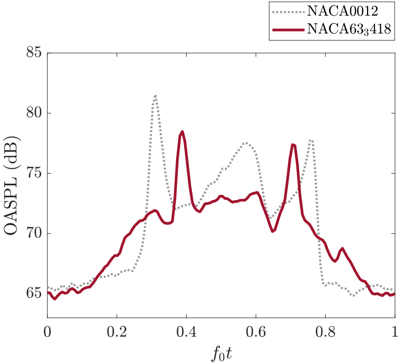

$$\mathrm{OASPL} = 10 \log_{10} \left(\frac{1}{p_{ref}^2} \int_{70\,\mathrm{Hz}}^{1000\,\mathrm{Hz}} S_{pp}(f) df \right)$$

- Maxima of noise at **stall onset** and at **flow reattachment.**

Perspectives (PhD Lisa Sicard)

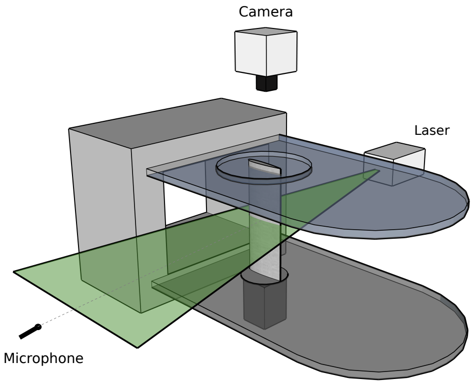

Synchronized acoustic/PIV measurements :

Sampling frequencies :

- PIV : $f_{\mathrm{PIV}} = 3$ kHz
- Microphones : $f_s = 51.2$ kHz

Objectives :

- Identify the flow structures responsible for the noise radiation
- Propose a model of dynamic stall noise

Wind turbine propagation effects

- Reflection over an impedance ground
- Refraction due to wind speed and temperature gradients
- Scattering due to atmospheric turbulence
- Effect of topography
- Effect of wind turbine wakes

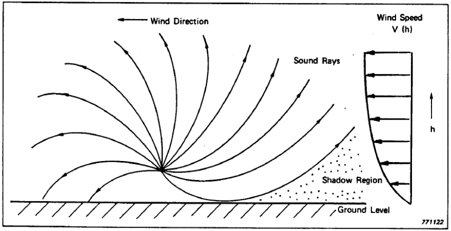

Lamancusa [2009]

We focus on the effect of the source modelling over a flat and homogeneous ground in a neutral atmosphere :

$$\bar{u}(z) = \frac{u_*}{\kappa} \ln\left(\frac{z}{z_0}\right)$$

$$\bar{T}(z) = T_0 + \alpha_0 z \quad \text{with} \quad \alpha_0 \approx -0.01 \text{ K/m}$$

Wind turbine propagation effects

- Reflection over an impedance ground
- Refraction due to wind speed and temperature gradients
- ~~Scattering due to atmospheric turbulence~~
- ~~Effect of topography~~
- ~~Effect of wind turbine wakes~~

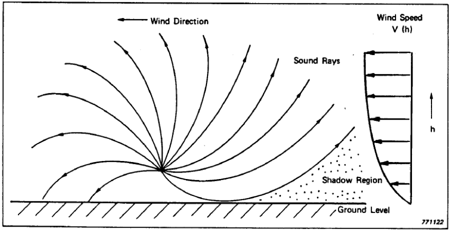

Lamancusa [2009]

We focus on the effect of the source modelling over a flat and homogeneous ground in a neutral atmosphere :

$$\bar{u}(z) = \frac{u_*}{\kappa} \ln\left(\frac{z}{z_0}\right)$$

$$\bar{T}(z) = T_0 + \alpha_0 z \quad \text{with} \quad \alpha_0 \approx -0.01 \text{ K/m}$$

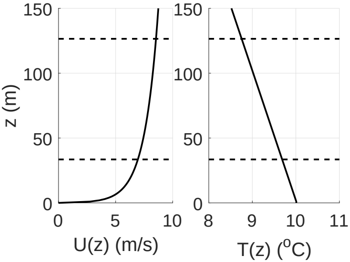

Point source approximation

Wind turbine represented as a monopole located at hub height

Ray-tracing example by Prospathopoulos and Voutsinas [2005]

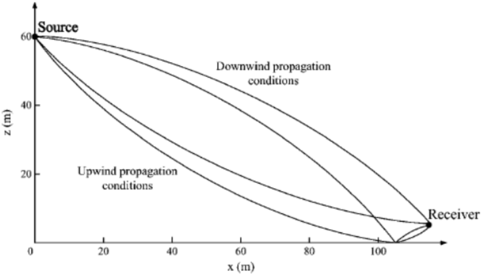

Fig. 13 Downward and upward refraction of eigenrays for downwind and upwind propagation conditions, respectively.

Link between sound power level $L_W(f)$ and sound pressure level $L_p(f)$

$$L_p(f) = L_W(f) - \underbrace{10\log_{10}(4\pi R_1^2)}_{\text{geometrical spreading}} - \underbrace{\alpha(f)R_1}_{\text{atmospheric absorption}} + \underbrace{\Delta L}_{\text{propagation effects}}$$

ΔL can be calculated with any propagation model

Extended source model using moving monopoles

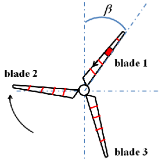

Point source approximation

For each segment and each angular position :

$$L_p(f,\beta) = L_W(f,\beta) - 10\log_{10}(4\pi R_1^2) + \Delta L(f) - \alpha(f)R_1$$

- angle-dependent sound power level $L_W(f,\beta)$ obtained from Amiet model
- $\Delta L(f)$ obtained from a set of parabolic equation (PE) calculations at N_h different heights

  $\Rightarrow$ closest point interpolation based on the segment height at angle β
- N_h PE calculations per frequency and per propagation direction

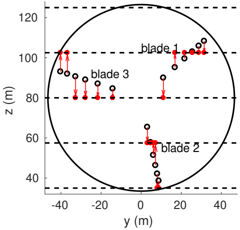

More details in Cotté, "Extended source models for wind turbine noise propagation", *Journal of the Acoustical Society of America* 2019.

Validation test cases

- 2.3 MW wind turbine with tower height 80 m
- variable porosity impedance model for a natural ground (Dragna *et al.*, 2015)
- test-case 1 : only trailing edge noise and homogeneous conditions ($c(z) = c_0$)

$\Rightarrow$ reference solution based on image source

- test-case 2 : both source mechanisms and profiles of $T(z)$ and $U(z)$ in a neutral atmosphere

Calculation parameters :

- 49 frequencies between 100 Hz and 2000 Hz
- domain : 1200 m along x and 300 m along z
- 30 angular positions β
- N_h varied between 1 and 19

Validation test cases

- 2.3 MW wind turbine with tower height 80 m
- variable porosity impedance model for a natural ground (Dragna *et al.*, 2015)
- test-case 1 : only trailing edge noise and homogeneous conditions ($c(z) = c_0$)

$\Rightarrow$ reference solution based on image source

- test-case 2 : both source mechanisms and profiles of $T(z)$ and $U(z)$ in a neutral atmosphere

Calculation parameters :

- 49 frequencies between 100 Hz and 2000 Hz
- domain : 1200 m along x and 300 m along z
- 30 angular positions β
- N_h varied between 1 and 19

Horizontal directivity of OASPL and AM in homogeneous conditions

Overall SPL averaged over one rotation (OASPL)

Amplitude Modulation : $\mathrm{AM} = \max_{\beta} \mathrm{OASPL}(\beta) - \min_{\beta} \mathrm{OASPL}(\beta)$

Directivity at $x = 1000\,\mathrm{m}$ and $z = 2\,\mathrm{m}$

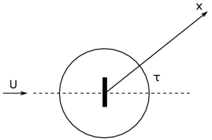

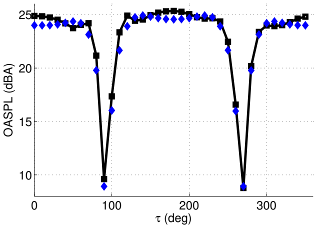

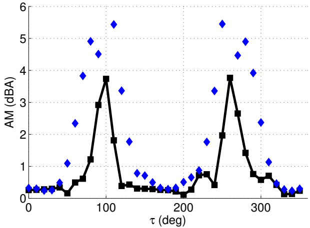

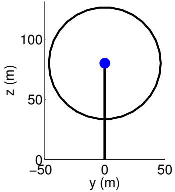

- Large errors with point source approximation

Horizontal directivity of OASPL and AM in homogeneous conditions

Overall SPL averaged over one rotation (OASPL)

Amplitude Modulation : $\text{AM} = \max\limits_{\beta} \text{OASPL}(\beta) - \min\limits_{\beta} \text{OASPL}(\beta)$

$\boxed{\text{Directivity at } x = 1000\,\text{m and } z = 2\,\text{m}}$

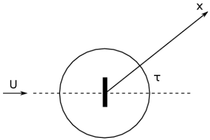

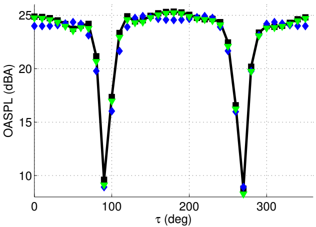

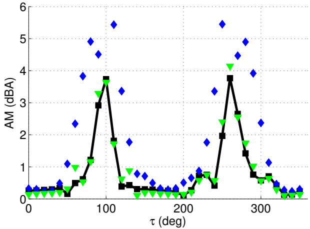

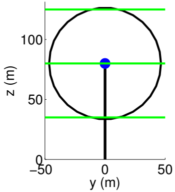

- Large errors with point source approximation

Horizontal directivity of OASPL and AM in homogeneous conditions

Overall SPL averaged over one rotation (OASPL)

Amplitude Modulation : $\mathrm{AM} = \max_{\beta} \mathrm{OASPL}(\beta) - \min_{\beta} \mathrm{OASPL}(\beta)$

Directivity at $x = 1000$ m and $z = 2$ m

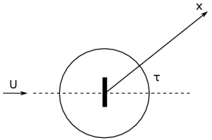

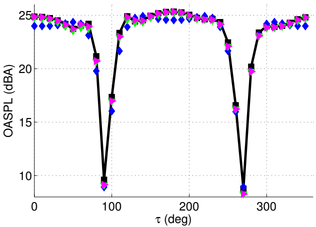

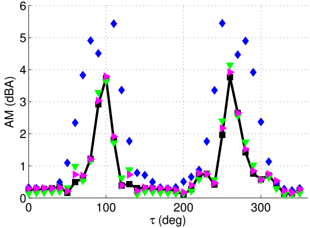

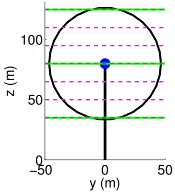

- Large errors with point source approximation
- Excellent results with $N_h = 7$ heights

Pressure maps in a neutral atmosphere

Difference between extended source model and point source approximation for $\tau = 180^o$

Extended source

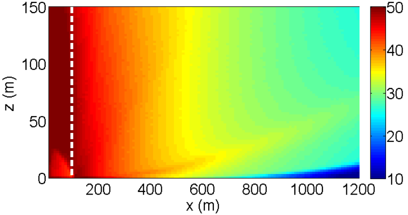

Point source

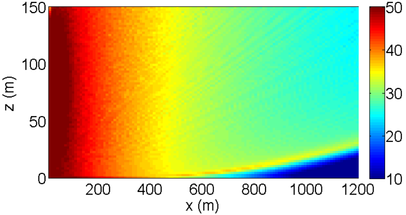

Horizontal directivity of OASPL and AM in a neutral atmosphere

Overall SPL averaged over one rotation (OASPL)

Amplitude Modulation : $\mathrm{AM} = \max_{\beta} \mathrm{OASPL}(\beta) - \min_{\beta} \mathrm{OASPL}(\beta)$

Directivity at $x = 1000\,\mathrm{m}$ and $z = 2\,\mathrm{m}$

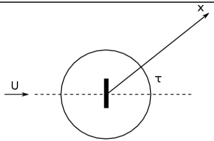

- $N_h = 19$ heights (—)
- $N_h = 10$ heights (■)
- $N_h = 3$ heights (△)
- point source approximation (- -)

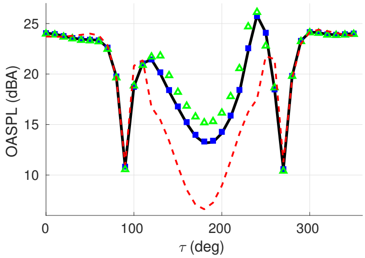

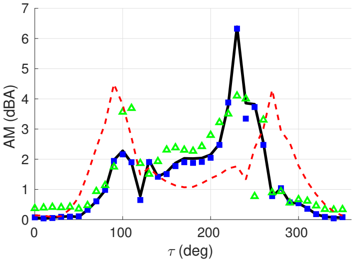

Some perspectives

- Compare model predictions with *in situ* measurements from the ANR PIBE project

  $\Rightarrow$ collaboration with David Ecotière and Benoit Gauvreau from UMRAE

- Account for propagation effects in the VRACE auralization tool (PhD David Mascarenhas)

  $\Rightarrow$ how to account for the phase and amplitude modulation associated with atmospheric turbulence ?

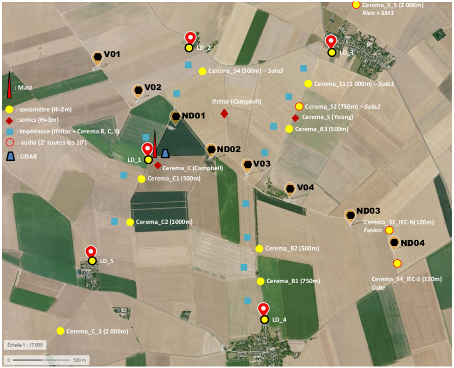

experimental campaign of ANR PIBE project with UMRAE